Integrin signaling is critical for pathological angiogenesis

Ganapati H. Mahabeleshwar,[1] Weiyi Feng,[1] David R. Phillips,[2] and Tatiana V. Byzova[1]

[1]Department of Molecular Cardiology, Joseph J. Jacobs Center for Thrombosis and Vascular Biology, NB50, The Cleveland Clinic Foundation, Cleveland, OH 44195
[2]Portola Pharmaceuticals Incorporated, South San Francisco, CA 94080

The process of postnatal angiogenesis plays a crucial role in pathogenesis of numerous diseases, including but not limited to tumor growth/metastasis, diabetic retinopathy, and in tissue remodeling upon injury. However, the molecular events underlying this complex process are not well understood and numerous issues remain controversial, including the regulatory function of integrin receptors. To analyze the role of integrin phosphorylation and signaling in angiogenesis, we generated knock-in mice that express a mutant β_3 integrin unable to undergo tyrosine phosphorylation. Two distinct models of pathological angiogenesis revealed that neovascularization is impaired in mutant β_3 knock-in mice. In an ex vivo angiogenesis assay, mutant β_3 knock-in endothelial cells did not form complete capillaries in response to vascular endothelial growth factor (VEGF) stimulation. At the cellular level, defective tyrosine phosphorylation in mutant β_3 knock-in cells resulted in impaired adhesion, spreading, and migration of endothelial cells. At the molecular level, VEGF stimulated complex formation between VEGF receptor-2 and β_3 integrin in wild-type but not in mutant β_3 knock-in endothelial cells. Moreover, phosphorylation of VEGF receptor-2 was significantly reduced in cells expressing mutant β_3 compared to wild type, leading to impaired integrin activation in these cells. These findings provide novel mechanistic insights into the role of integrin–VEGF axis in pathological angiogenesis.

CORRESPONDENCE
Tatiana V. Byzova:
byzovat@ccf.org

Abbreviations used: EC, endothelial cell; ERK, extracellular signal–regulated kinase; VEGF, vascular endothelial growth factor; VEGFR, vascular endothelial growth factor receptor; von Willebrand factor, vWF.

The process of angiogenesis involves coordinated endothelial cell (EC) proliferation, invasion, migration, and tube formation. This process is induced by vascular growth factors in coordination with extracellular matrix–interacting molecules such as integrins (1). Among integrins, $\alpha_v\beta_3$ heterodimer is known to be up-regulated on proliferating endothelial cells during angiogenesis and vascular remodeling. The disruption of $\alpha_v\beta_3$ integrin ligation by either blocking antibodies or cyclic peptide antagonists prevented blood vessel formation in mouse retina, rabbit cornea, chick chorioallantoic membrane, and human skin transplanted onto athymic mice (2–6). Histological examination of tumor tissue from mice treated with the $\alpha_v\beta_3$ blockers revealed reduction in the tumor cell viability and in the vascular density (7). These findings suggested that integrin $\alpha_v\beta_3$ provides cellular signals that facilitate EC proliferation and migration during angiogenesis.

However, studies using β_3- and β_5-null mice demonstrated enhanced tumor growth, tumor angiogenesis, and vascular endothelial growth factor (VEGF)-A–induced vascular permeability caused by elevated levels of VEGF receptor (VEGFR)-2 on ECs (8, 9). Therefore, it has been concluded that $\alpha_v\beta_3$ and $\alpha_v\beta_5$ integrins function as negative regulators of angiogenesis by restricting the VEGFR-2 expression (10). Surprisingly, neither $\alpha_v\beta_3$ blocking antibody nor cyclic peptide antagonists induced VEGFR-2 expression in any of the model systems described in previous studies. This raises the possibility that an enhanced expression of VEGFR-2 in integrin β_3/β_5–deficient mice could be a result of over-compensation because both integrins are pivotal for early embryonic vasculogenesis and angiogenesis (11). Another hypothesis suggested by authors of previous studies is that unligated integrins can act as negative regulators of cell survival by initiating a process referred to as "integrin-mediated cell death." Therefore, a genetic ablation of a proapoptotic stimulus (i.e., unligated $\alpha_v\beta_3/\alpha_v\beta_5$) would lead to increased endothelial cell survival in vivo, contributing to increased blood vessel density (12). Overall, because

of the great deal of controversy, the precise role of $\alpha_v\beta_3$ integrin in endothelial cell biology and angiogenesis remains unclear.

One of the characteristic features of integrins is the ability to transduce signals through the cellular membrane in both directions. Outside-in signaling informs the cell about the extracellular matrix environment. Inside-out signaling, known as integrin activation, is the process stimulated by agonist (i.e., thrombin or adenosine diphosphate for platelets and growth factor for EC) and results in changes in integrin functional activity (13). The cytoplasmic domains of integrins play a vital role in these bidirectional signaling processes. The cytoplasmic domain of the β_3 subunit of the vitronectin receptor ($\alpha_v\beta_3$) undergoes phosphorylation in response to cell adhesion to an immobilized ligand (14). Phosphorylated β_3 can recruit signaling intermediates, Shc and GRB2, suggesting that the phosphorylation of the β_3 cytoplasmic domain may induce Ras activation in several cell types (15).

To elucidate the role of β_3 integrin and its complexes, we characterized mice that express a mutant form of β_3 integrin, but not the WT form (knock-in mice). In the mutant, the two tyrosine residues known to be involved in integrin signaling, Tyr747 and Tyr759, were substituted to phenylalanines. The mutant is unable to undergo phosphorylation of cytoplasmic domain, resulting in deficient integrin signaling. In these mice, named DiYF, the mutant β_3 integrin is physically present on all cell types, which should prevent any developmental compensatory changes. Recent studies using DiYF mice demonstrated that mutation of both cytoplasmic tyrosine residues of the β_3 cytoplasmic domain leads to the defective function of $\alpha_{IIb}\beta_3$ on platelets, unstable platelet aggregation, and clot retraction in vitro and to an enhanced tendency to rebleed in vivo (16, 17). Thus, although it is clear that β_3 integrin cytoplasmic tyrosine motifs play an important role in integrin signaling in platelets, its function in endothelial and other specialized cells remains unknown.

In the specialized cells, integrins form functional complexes with other receptors on the cell surface. Most often, integrins are associated with tyrosine kinase receptors and these two types of receptors influence each others activity (18, 19). On ECs, $\alpha_v\beta_3$ integrin is intimately linked with the VEGFR-2, because VEGF is able to induce $\alpha_v\beta_3$ integrin expression and activation (20). At the same time, $\alpha_v\beta_3$ is able to enhance the phosphorylation of VEGFR-2 in response to VEGF and subsequent activation of SAPK2/p38 and FAK.

We sought to directly establish the role of β_3 integrin tyrosine phosphorylation and integrin signaling in VEGF-stimulated responses of EC and in pathological angiogenesis in vivo. To this end, we combined in vivo and ex vivo angiogenesis assays with an extensive characterization of ECs derived from both WT and DiYF mice to perform a complete analysis of the role of integrin β_3 and its signaling in functional responses to VEGF.

RESULTS

In ECs, tyrosine phosphorylation of β_3 cytoplasmic domain occurs upon adhesion to integrin ligands

Previous studies using cell lines and platelets demonstrated that phosphorylation of β_3 integrin cytoplasmic tyrosines is involved in outside-in integrin signaling. Therefore, we assessed whether EC adhesion to extracellular matrix proteins could induce tyrosine phosphorylation of β_3 integrin. We isolated ECs from the lungs of WT and DiYF mice, plated them on various substrates, and assessed the phosphorylation of β_3 integrin on Tyr747 and Tyr459 (Fig. 1, A and B). Very low levels of phosphorylation of WT β_3 integrin were observed when cells were kept in suspension or plated on poly-L-lysine. Extracellular matrix proteins that serve as ligands for $\alpha_v\beta_3$ such as vitronectin, fibronectin, fibrinogen, and gelatin strongly stimulated Tyr759 and Tyr747 phosphorylation of WT ECs. Laminin and collagen, which are recognized primarily by integrins other than $\alpha_v\beta_3$, induced lower levels of tyrosine phosphorylation. Sodium pervanadate, known to block phosphatase activity, was used as a positive control in this experiment. As anticipated, no tyrosine phosphorylation of β_3 integrin was observed in DiYF EC under any conditions.

VEGF treatment of ECs induces tyrosine phosphorylation of β_3 integrin

The role of the β_3 subunit phosphorylation in extracellular matrix recognition was previously assessed in CHO cells and K562 cells. These systems do not provide insight into the roles of β_3 integrin in angiogenesis and in the regulation of VEGF or FGF-induced EC responses. These processes can be only assessed in ECs expressing appropriate receptors and signaling intermediates. We sought to determine whether VEGF treatment affected the phosphorylation status of β_3 integrin. Treatment of ECs with VEGF-A165 induced both Tyr747 and Tyr759 phosphorylation in a time-dependent manner (Fig. 1 C). Both time curves of β_3 tyrosine phosphorylation followed a bell-shaped pattern, which is typical for growth factor–induced responses. Thus, not only integrin engagement, but also VEGF treatment stimulated tyrosine phosphorylation of β_3 subunit in ECs, suggesting a possible regulatory role for this process in VEGF-induced angiogenesis.

Pathological angiogenesis is impaired in DiYF mice

We next evaluated whether β_3 integrin cytoplasmic tyrosine motifs are crucial for a complete angiogenic response to VEGF in vivo. We implanted VEGF-A–containing Matrigel subcutaneously into WT and DiYF mice and assessed the angiogenic response based on the amount of hemoglobin extracted from Matrigel. As shown in Fig. 2 A, the hemoglobin concentration was at least fivefold lower in Matrigel plugs isolated from DiYF mice compared with WT counterparts. The vascular density in Matrigel implants was assessed by von Willebrand factor (vWF) staining. Only 50% of Matrigel plugs from DiYF mice had a distinguishable vasculature and
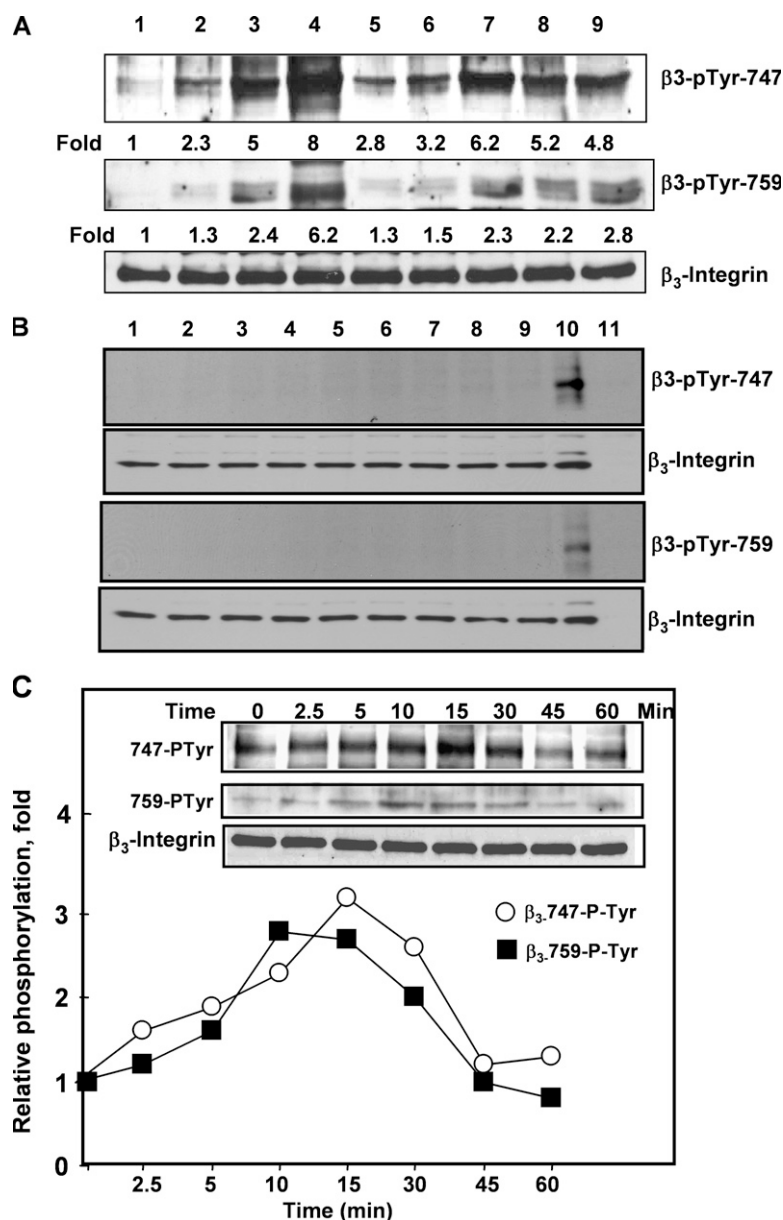
Figure 1. Extracellular matrix proteins and VEGF induce β₃ in–tegrin cytoplasmic tyrosine phosphorylation. WT (A) and DiYF (B) cells were held in suspension (lane 1); plated on poly L-lysine (lane 2); gelatin, with (lane 4) or without (lane 3) pervanadate treatment; or laminin (lane 5), collagen (lane 6), vitronectin (lane 7), fibronectin (lane 8), or fibrinogen (lane 9) and incubated at 37°C for 60 min. Cell lysates were subjected to Western blot analysis using anti–integrin β₃ [pY747] antibody (A and B, top) or [pY759] antibody (A and B, middle). WT cells plated on vitronectin and CHO cell lysates were used as positive and negative control, respec-tively in panel B (lanes 10 and 11). Cell lysates were also analyzed for β₃ integrin expression as a loading control (A and B, bottom). (C) VEGF in-duces β₃ integrin tyrosine phosphorylation. WT and DiYF mouse lung ECs were treated with 20 ng/ml of VEGF-A165 for 0–60 min. Phosphorylation statuses of β₃Y747 (top) and β₃Y759 (middle) were assessed as described in Materials and methods. The amount of β₃ integrin in all samples was quantitated by anti–β₃ integrin antibody (bottom). Densitometry analysis was performed, and fold changes over control are shown.

exhibited staining for vWF (Fig. 2 B, top). The vascular density was 4.2-fold lower in DiYF mice than in WT controls (P = 0.01) (Fig. 2 B, bottom). Thus, VEGF–induced angio-genesis was significantly impaired in DiYF mice.

Further, we assessed tumor-induced pathological angio-genesis in DiYF and WT mice. To this end, mouse melanoma cells (B16F10) were implanted subcutaneously into mice, and after 10 d tumors were excised. The average weight of tu-mors formed in DiYF mice was at least twofold lower than average tumor weight in WT mice (0.14 g vs. 0.29 g) (Fig. 2 C). Tissue section analysis revealed the presence of well-developed blood vessels that stained positively for CD31, and
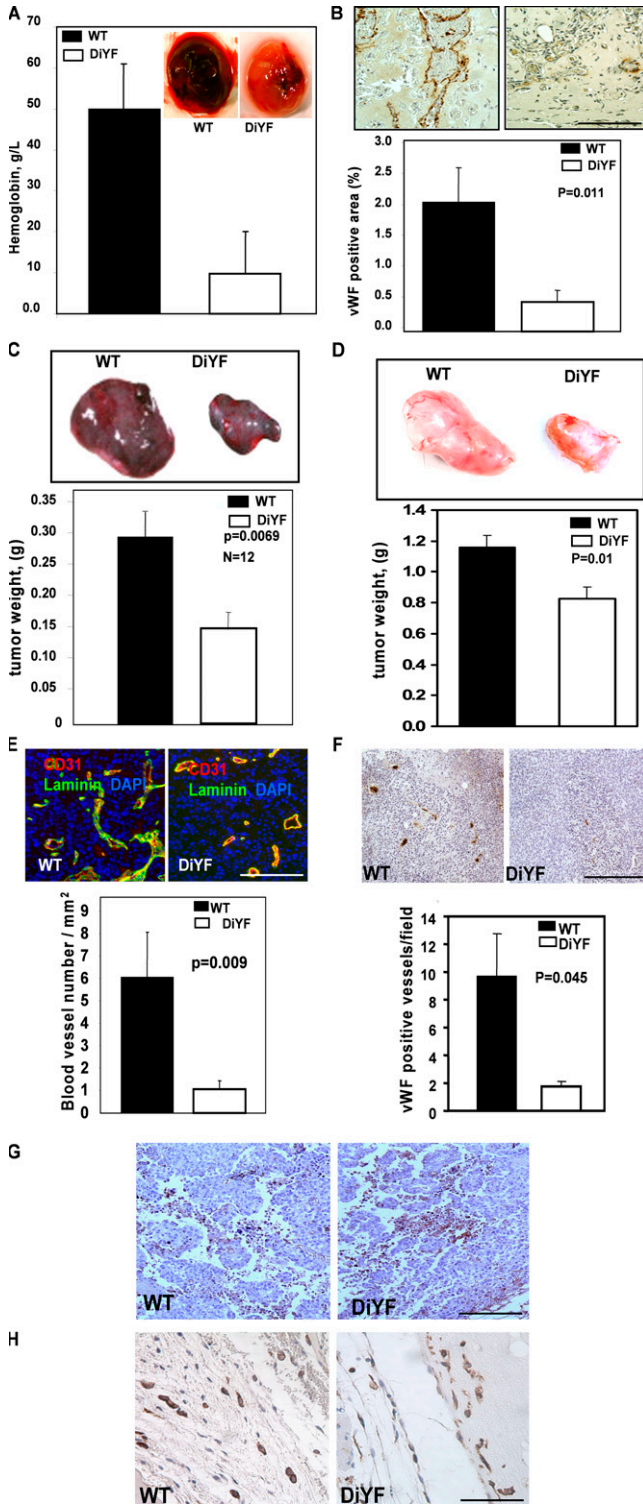
Figure 2. VEGF–induced angiogenesis is impaired in DiYF mice.
(A) WT and DiYF mice were injected subcutaneously with Matrigel containing VEGF. Hemoglobin content of Matrigel pellets in WT or DiYF mice was measured with the Drabkin reagent. (B) Representative light microscopic pictures of Matrigel implant sections stained with vWF antibody from WT and DiYF mice. The areas positive for vWF antibody staining, as a percentage of total Matrigel cross-sectional area, were measured from each plug

laminin in tumors from WT mice. In contrast, in tumors formed in DiYF mice, blood vessels were sparse and thin walled based on laminin staining (Fig. 2 E, top). The vascular density in tumors grown in DiYF mice was sixfold lower than that in WT mice ($P = 0.009$) (Fig. 2 E, bottom). Similar defects in tumor growth and neovascularization were observed using alternative model of tumor growth in vivo. Mouse prostate cancer cells (RM-1) were implanted into WT and DiYF mice, and tumor was excised after 10 d. Tumors formed in DiYF mice were smaller than in WT mice (1.17 g vs. 0.8 g) (Fig. 2 D). Tissue section analysis indicated the presence of substantially larger number of vWF-positive blood vessels in tumor developed in WT mice compared with DiYF mice (Fig. 2 F). Collectively, our in vivo studies demonstrate that tumor angiogenesis is impaired in DiYF mice, resulting in reduced tumor growth. Thus, it appears that β_3 integrin cytoplasmic tyrosine motifs play crucial role in the regulation of pathological angiogenesis.

Knowing that monocytes/macrophages use β_3 integrin for their arrest and extravasation at sites of inflammation, we assessed whether DiYF mutation affects macrophage recruitment into tumors using anti–F4/80 antibody staining. As shown in Fig. 2 G, considerable amounts of macrophages were found to be present in tumors implanted in both WT and DiYF mice. No substantial reductions in macrophage recruitment were found in DiYF mice. Similar results were observed in Matrigel model of VEGF–induced angiogenesis (Fig. 2 H). Thus, DiYF mutations within β_3 integrin do not impair the process of macrophage recruitment in tumors.

Normal embryogenesis and adult vasculature development in DiYF mice

Homozygous WT and DiYF mice were bred to obtain homozygous littermates. The average number of embryos per litter was the same. Size and weight of pups were not substantially different between WT and DiYF mice. In contrast to β_3 integrin knockout mice, no embryonic mortality caused by placental defects was observed in DiYF mice. DiYF mutation did not affected survival of embryos at early stages of development. DiYF embryos did not exhibit any broad vascular defects (Fig. 3 A). Prenatal DiYF mutant mothers

section. Bar, 10 μm. (C–F) Functional β_3 integrin is essential for enhanced pathological angiogenesis. B16F10 mouse melanoma (C) and RM1 mouse prostate carcinoma (D) cells were implanted subcutaneously in WT and DiYF mice, and tumors were excised after 10 d. Representative melanoma (C) and prostate carcinoma (D) tumors formed in WT and DiYF are shown. Weights of tumors grown in WT and DiYF mice were measured and represented in the bar graph. (E) Tumor sections were stained with anti–mouse CD31 and antilaminin antibodies. The positively stained blood vessels were counted, and results are shown in the bar graph. Bar, 80 μm. (F) RM1 tumor sections were stained by anti-vWF antibody. The stained blood vessels were counted and represented in the bar graph. Bar, 220 μm. (G–H) Macrophage infiltration at the site of angiogenesis in DiYF mice. B16F10 tumor (G) and Matrigel (H) sections were stained with macrophage marker F4/80. Bars: (G) 80 μm; (H) 40 μm.
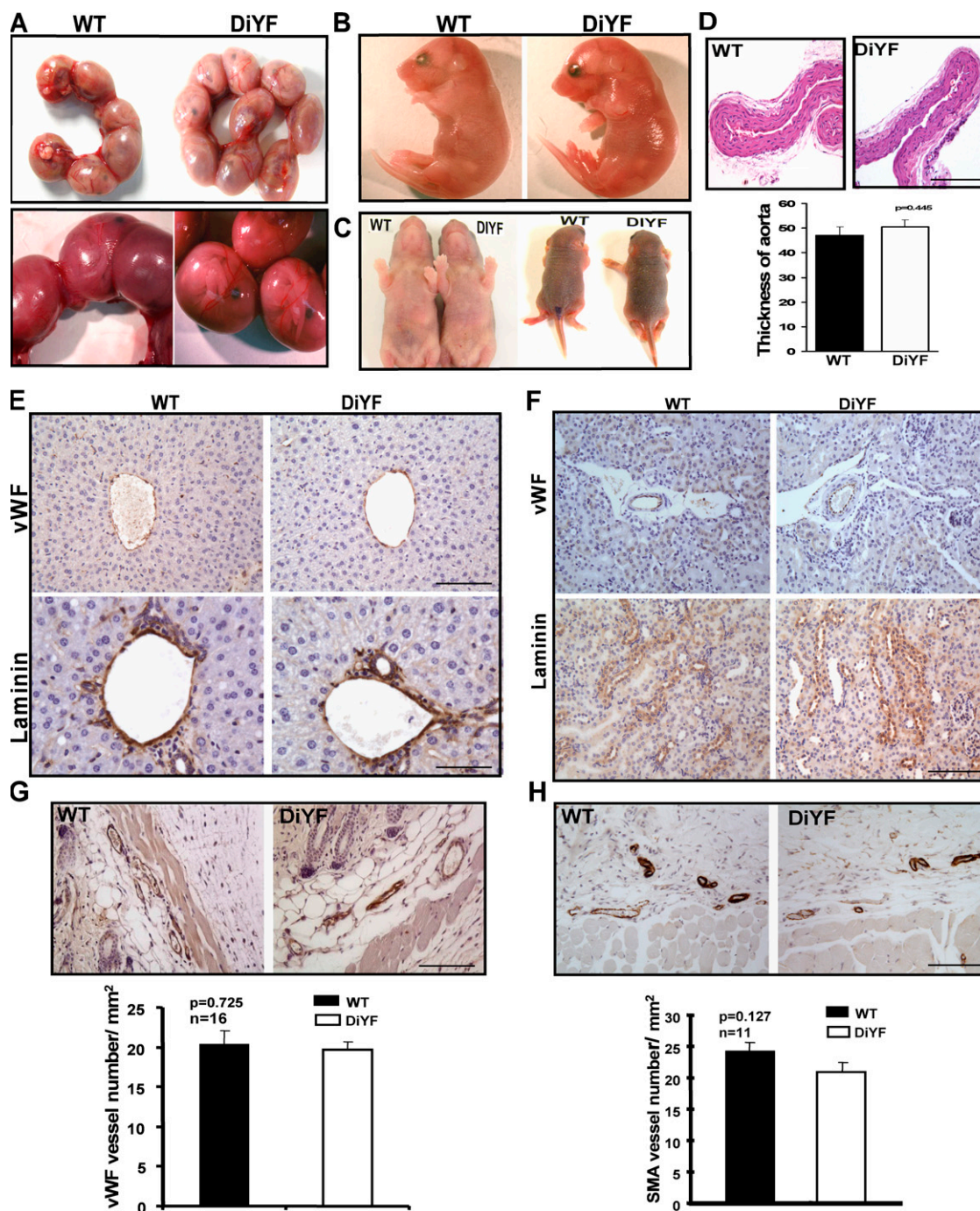
Figure 3. Embryogenesis and vascular phenotypes are broadly normal in adult DiYF mice. (A) Uteri from WT and DiYF females that has been bred to WT and DiYF males, respectively. DiYF uteri were completely normal and did not show any kind of vascular defects or hemorrhage. (B) Homozygous E14 embryos from uterus were normal and did not show any differential mortality. (C) 2-d-old typical homozygous WT or DiYF pups did not show any differential mortality or vascular defects. (D) Aortas from WT and DiYF mice were fixed with formalin and embedded in paraffin. The thickness of aortas was measured and represented in the bar diagram. Bar, 180 μm. (E–F) Livers and kidneys from WT and DiYF mice were fixed and embedded in paraffin. Tissue sections were stained by with anti-vWF and anti-laminin antibody. Bars: (E, top) 100 μm; (E, bottom) 50 μm; (F) 100 μm. (G and H) WT and DiYF skin samples were fixed and embedded in paraffin. Representative tissue sections stained with anti-vWF (G) and anti-SMA (H) antibodies are shown. Bars, 100 μm. Positively stained blood vessels were counted and represented in bar graphs.
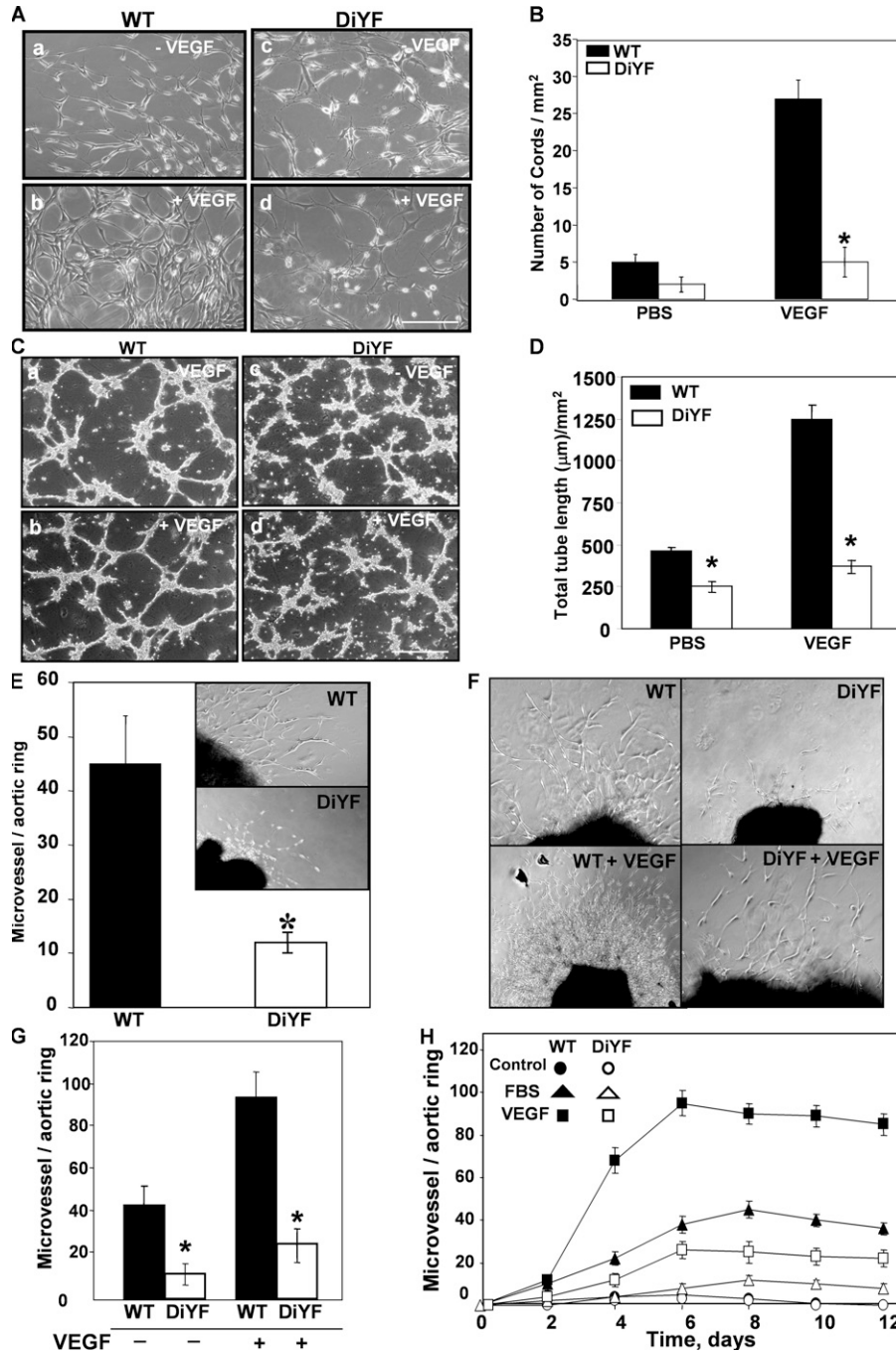
Figure 4. β₃ integrin tyrosine 747 and 759 mutations impair ang-iogenic properties of ECs. (A and B) Functional β_3 integrin is essential for endothelial cell organization into precapillary cords. WT and DiYF mouse lung endothelial cells were seeded on Matrigel-coated plates and cells were allowed to adhere. After 24 h, cells were overlaid with Matrigel with or without VEGF and maintained in culture. (A) Three random fields were photographed periodically using phase–contrast microscope. Bar, 200 μm. (B) Quantification of cords numbers per field (*, P = 0.0004). (C and D) β_3 integrin cytoplasmic tyrosine residues are critical for capillary tube formation. Single cell suspensions of WT and DiYF mouse lung ECs were transferred to Matrigel-coated plates and incubated with or without VEGF. (C) Endothelial capillary tubes formed in Matrigel were photographed. Bar, 200 μm. (D) The length of tubes in random fields from each well was analyzed using ImagePro software (*, P < 0.0005). (E) β_3 integrin cytoplasmic tyrosine motifs are required for normal microvessel growth. WT and DiYF mouse aortic rings were embedded in Matrigel and main-tained at 37°C for 6 d. Microvessel outgrowths from aortic rings were observed periodically and photographed. Numbers of microvessel sprouts from aortic rings were counted and represented in the bar graph. *, P = 0.00046. (F) Defective β_3 integrin tyrosine phosphorylation reduces VEGF-induced microvessel outgrowth. WT and DiYF mouse aortic rings were im-planted in Matrigel with or without VEGF and maintained under aseptic condition for 6 d. Microvessel growth from implants was observed peri-odically and microphotographed. (G) The number of microvessel outgrowth from aortic implants was counted and shown in G. *, P < 0.0005. (H) The ex vivo aortic ring assay using WT and DiYF aortic rings was performed in

did not suffer from intrauterine hemorrhage and placental defects (Fig. 3 B) as observed in β_3 integrin knockout mice. To examine the survival of DiYF mutant mice after birth, the numbers of pups per litter from homozygous crosses were monitored. Even after 7 d of postpartum there was no significant difference in mortality of pups between these two groups. The DiYF mutant embryos (P = 12) or pups did not show any vasculature defects and hemorrhage in skin or in gastrointestinal tract as observed in β_3 integrin knockout mice (Fig. 3 C). Development of large blood vessels exemplified by aorta also appeared to be normal because no significant differences (P = 0.445) in thickness and general histological structures of aorta were observed in DiYF mice compared with WT counterparts (Fig. 3 D).

To further investigate the effect of DiYF mutation on adult vasculature, tissue sections of liver (Fig. 3 E) and kidney (Fig. 3 F) were stained for vWF and laminin. No substantial differences in blood vessel density of vascular maturation were observed in DiYF mice. Vascular density was assessed in skin sections from WT and DiYF mice using staining for vWF, and there were no significant differences between these two groups (P = 0.725, n = 16; Fig. 3 G). Since vascular maturation and pericyte recruitment are known to be essential for pathological angiogenesis (21), staining for smooth muscle actin was performed to reveal mature blood vessels (Fig. 3 H). Quantitative results demonstrate the similar density of smooth muscle actin–positive blood vessels in skins of WT and DiYF mice (P = 0.127; n = 11). Since β_3 integrin is known to be expressed on circulating white blood cells and involved in immune response, we demonstrated that the numbers of circulating immune cells do not differ among DiYF and WT mice. The numbers of circulating lymphocytes were 86.5 ± 0.93 and 80.1 ± 2.7 × 10^3 cells/μl for WT and DiYF mice, respectively. Monocyte counts were also similar: 2.34 ± 0.5 and 2.32 ± 0.6 × 10^3 cells/μl for WT and DiYF mice, respectively. Collectively, these data clearly indicate that DiYF mutation did not affect the embryogenesis, organogenesis, postpartum developments, normal vascular development and maturation, and levels of circulating white blood cells.

DiYF mutations within the β_3 integrin cytoplasmic domain impair angiogenic properties of ECs

Previous studies demonstrated that $\alpha_v\beta_3$ integrin controls migration, invasive potential, and angiogenic phenotype of ECs (20). Therefore, we assessed whether impaired β_3 integrin tyrosine phosphorylation affected EC capillary and tube formation ex vivo. WT but not DiYF ECs were able to form well-assembled and complete capillary cord–like structures in the presence of VEGF-A (Fig. 4 A). In contrast, DiYF ECs

remained randomly scattered without any signs of organization (Fig. 4 A). The number of cords formed by WT EC was 5.4-fold higher compared with DiYF cells (Fig. 4 B).

A major phenotypic characteristic of ECs is the ability to assemble into the interconnected network of tube-like structures when grown in a three-dimensional matrix (22). WT but not DiYF ECs formed clearly defined and well-connected networks of EC tubes (Fig. 4 C). These structures were relatively stable and remained well organized for at least 18 h. As evident from Fig. 4 C, DiYF ECs were not able to complete tube formation, and no obvious patterns were formed even in the presence of VEGF. The extent of tube formation was quantified by measuring the length of tubes; the mean values of three independent experiments are represented graphically in Fig. 4 D. VEGF treatment induced approximately threefold increase in the length of the tubes formed by WT ECs but had a little effect on DiYF ECs.

β_3 integrin cytoplasmic tyrosine motifs controls ex vivo angiogenesis in response to VEGF

We next assessed whether DiYF mutations affected an outgrowth of vascular sprouts from aortic segments isolated from mice. First, an ex vivo angiogenic assay was performed in Matrigel enriched with growth factors. The aortic rings from WT mice produced an extensive network of vascular sprouts, whereas DiYF aortic rings failed to do so (Fig. 4 E). To elucidate the role of β_3 integrin in VEGF-induced responses, the aortic ring assay was performed in the presence or absence of VEGF using growth factor–reduced Matrigel. Under these conditions, aortic rings from WT mice produced a significantly higher number of vascular sprouts both in the absence and presence of VEGF than did aortic rings from DiYF mice (Fig. 4 F). Quantification of the number of aortic ring sprouts indicated that DiYF cells formed fourfold fewer vascular sprouts ex vivo, regardless of stimulation, than did WT aortic rings (Fig. 4 G). VEGF produced a small increase in capillary formation of DiYF rings; however, the number of sprouts was only 20–25% of that observed in WT aortic rings (Fig. 4 G).

To further analyze the capillary growth from aortic rings, a detailed kinetic study was undertaken. The time curves of vascular growth are presented in Fig. 4 H. In the absence of stimulation, very few microvessels were detected in either WT or DiYF implants even after a prolonged incubation, whereas serum-induced neovascularization was considerably higher in WT implants than in DiYF implants (Fig. 4 H). The peak values of capillary growth were observed 8 d after implantation and were 10 and 45 microvessels per ring for DiYF and WT, respectively. VEGF with endothelial growth supplement was a stronger stimulus than endothelial growth supplement alone, but both produced extensive formation of

---

the presence of DMEM without any supplements, with endothelial growth supplement, or with VEGF together with endothelial growth supplement. Aortic rings were observed every 2 d, numbers of sprouts from each implant were counted, and photographs were taken. Growth kinetics of WT

and DiYF aortic rings under various conditions were analyzed and the growth curves are shown. The data represents the results of three independent experiments performed in triplicate.

capillaries in WT but not in DiYF aortic rings (Fig. 4 H). Collectively, these results indicate that the impaired pathological angiogenesis in DiYF mice was caused by the defective functional responses of endothelial cells.

β_3 integrin cytoplasmic tyrosine motifs regulates EC adhesion, spreading, and migration

To further define the nature of the angiogenic defect observed in DiYF mice, we compared angiogenesis-relevant functions of ECs isolated from WT and DiYF mice. We first assessed whether the mutation in β_3 integrin cytoplasmic domain had any effect on EC adhesion and subsequent cell spreading on extracellular matrix substrates. WT and DiYF ECs were plated on various integrin ligands and numbers of attached and spread cells per field were counted. WT and DiYF ECs adhered and spread equally well on fibronectin, laminin–1, and collagen-coated plates (Fig. 5, A and B). In contrast, a significant difference (P < 0.001) in the behavior of WT and DiYF ECs was found using the $\alpha_v\beta_3$ ligands vitronectin and entactin. On these substrates, DiYF ECs showed a twofold reduction in adhesion and a fourfold decrease in the number of spread cells on vitronectin and threefolds on entactin (Fig. 5, A and B). To further examine the role of β_3 integrin cytoplasmic tyrosine motifs in regulation of receptor ligand-binding strength, we examined cell adhesion under conditions of shear stress. WT and excessive DiYF endothelial cells were plated on vitronectin–coated glass coverslips to achieve equal number of adherent cells. Then, adherent cells were subjected to perfusion with shear rates of 5–30 dyn/cm^2 for 1 min. As shown in Fig. 5 C, shear stress revealed a dramatic difference in strength of adhesion between WT and DiYF endothelial cells. Shear stress of 10 to 15 dyne/cm^2 almost completely abolishes DiYF endothelial cell adhesion to vitronectin, whereas >60% of WT endothelial cells remained tightly adhered to the matrix. Shear rate sufficient to wash away 50% of adherent cells was 23 and 8 dyne/cm^2 for WT and DiYF endothelial cells, respectively (Fig. 5 C). This finding demonstrates that β_3 integrin cytoplasmic tyrosine motifs regulates ligand-binding strength.

When the migratory activity of WT and DiYF ECs toward various extracellular matrix proteins known to be recognized by integrins was compared, results were similar to those of the adhesion assays: WT and DiYF ECs migrated equally well toward fibronectin, laminin, and collagen, but not toward vitronectin and entactin, where a 2.5-fold reduction in migration of DiYF ECs compared with WT was observed (Fig. 5 D).

We then compared the VEGF-induced migratory activity of WT and DiYF ECs. Stimulation of WT ECs with VEGF at 5, 10, and 20 ng/ml induced 1.5-, 2.5-, and 2.9-fold increases of migration compared with untreated ECs (Fig. 5 E). DiYF ECs also responded to VEGF stimulation; however, the rate of migration was substantially reduced when compared with WT cells (Fig. 5 E). Thus, tyrosine phosphorylation of $\alpha_v\beta_3$ integrin appears to play an important role in VEGF-induced EC migration to extracellular matrix. To further

confirm these results, we used an alternative and more physiologically relevant method to assess EC migration. WT and DiYF ECs were plated on various integrin ligands and were allowed to form a confluent monolayer. Then, a wound in the monolayer was created and the healing process was monitored at different time points. The quantitative aspects of wound recovery and representative images of ECs are presented in Fig. 5, F and G, respectively. Whereas WT and DiYF EC migrated equally well on fibronectin, laminin, and collagen, a threefold reduction in migration on vitronectin was observed in DiYF ECs compared with WT (Fig. 5 F). The DiYF mutation impairs $\alpha_v\beta_3$ integrin-dependent and VEGF-stimulated responses of ECs, underscoring the role of phosphorylation of tyrosines in the cytoplasmic domain in the regulation of a cross-talk between $\alpha_v\beta_3$ and VEGFRs.

β_3 integrin cytoplasmic tyrosine motifs are required for sustained activation of VEGFR–2

Next, we sought to identify a molecular mechanism responsible for abnormalities observed in DiYF ECs. Previous studies using β_3-null mice demonstrated that the absence of β_3 leads to up-regulation of VEGFR–2 and consequently to augmentation of angiogenic responses of ECs (8). However, no differences in VEGFR–2 levels were observed between DiYF and WT ECs from lung or aortic origin (unpublished data). It was previously shown that integrin β_3 forms a complex with VEGFR–2 immediately upon stimulation with VEGF, and this association was proposed to be necessary for the activation of angiogenic program in ECs (23). Therefore, we sought to determine whether the DiYF mutations impaired the interaction of β_3 integrin with VEGFR–2. Low levels of β_3–VEGFR–2 interaction were observed in unstimulated WT ECs in suspension or upon adhesion to extracellular matrix. VEGF stimulated a dramatic increase in formation of the complex between β_3 and VEGFR–2 in WT ECs plated on vitronectin, but not in suspension or on laminin, demonstrating the ligand specificity of this phenomenon (Fig. 6 A). In contrast, no interaction between β_3 and VEGR–2 was observed in DiYF ECs under any conditions (Fig. 6 B). Thus, β_3 tyrosine phosphorylation was essential for an interaction between VEGFR–2 and $\alpha_v\beta_3$ integrin.

To investigate the mechanism of β_3 integrin-dependent VEGF signaling, we analyzed the VEGFR–2 phosphorylation status in WT and DiYF ECs after VEGF stimulation. The time courses of VEGR–2 phosphorylation are shown in Fig. 6 C. In WT ECs, VEGF induced a bell- shaped response with a maximum sixfold increase in VEGFR–2 phosphorylation relative to unstimulated cells. After 45 min, VEGFR–2 phosphorylation returned to the control level. In contrast, the maximum VEGFR–2 phosphorylation in DiYF ECs upon VEGF stimulation was only 2.5-fold over control. Importantly, VEGFR–2 remained phosphorylated three times longer in WT ECs than in DiYF ECs (Fig. 6 C). Thus, the lack of integrin phosphorylation in DiYF ECs resulted in reduced phosphorylation, and therefore activation, of VEGFR–2 in response to VEGF, which in turn affected all the signaling
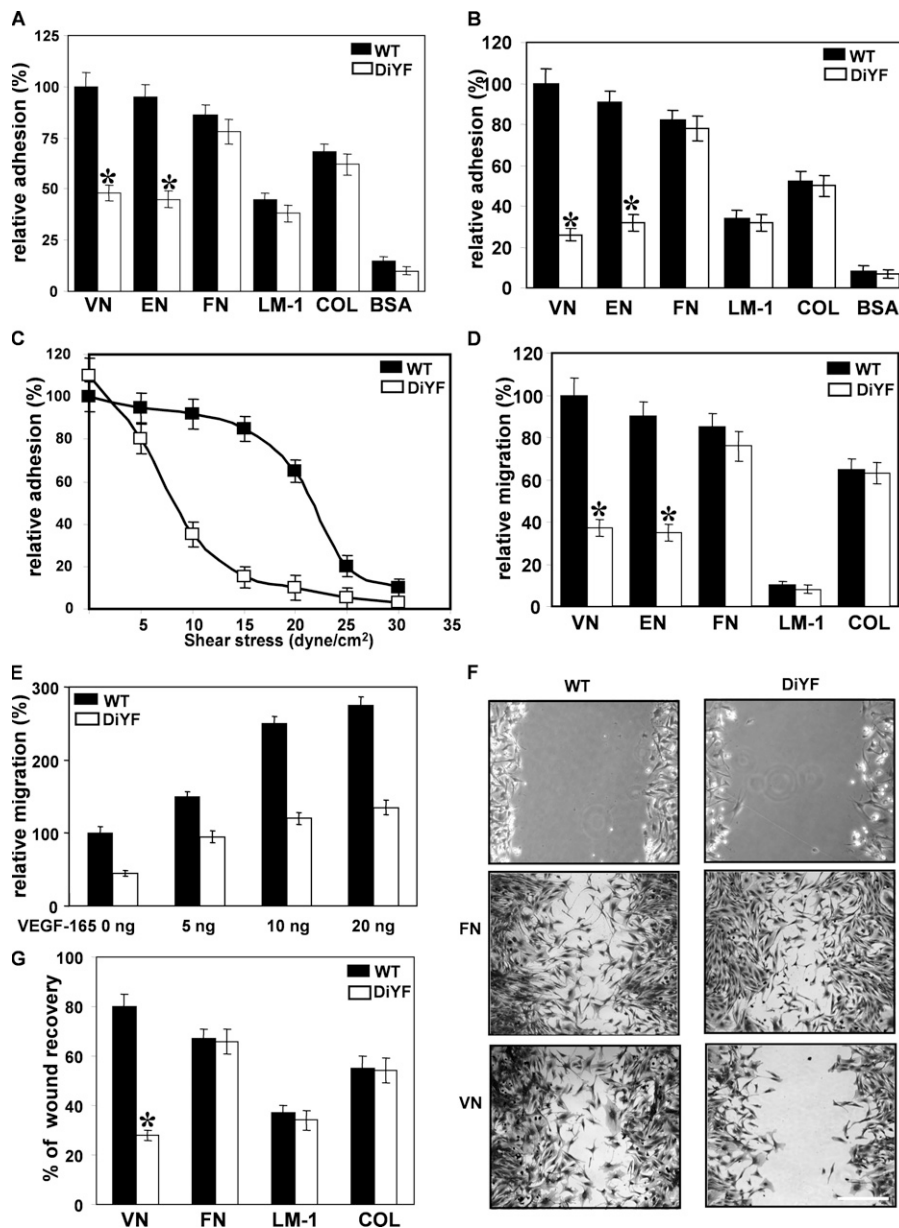
Figure 5. β₃ **integrin cytoplasmic tyrosine motif is critical for endo‐thelial cell adhesion, spreading, and migration.** (A and B) Adhesion and spreading of WT and DiYF endothelial cells on various integrin ligands. Plates were coated with vitronectin (VN), entactin (EN), fibronectin (FN), laminin-1 (LM-1), collagen (COL), or BSA. WT and DiYF mouse lung en‐dothelial cell suspensions were plated on each well coated with integrin ligands. Numbers of attached and spread cells per field were counted. Ad‐hesion and spreading of WT ECs on vitronectin was assigned a value of 100% (*, P = 0.000017 and 0.00003 for cell adhesion and spreading, re‐spectively). (C) β₃ integrin cytoplasmic tyrosine motifs regulate ligand bind‐ing strength. WT and 2.25-fold excess DiYF endothelial cells were added on vitronectin-coated coverslips to achieve equal number of adherent cells. Shear stress of 5–30 dyne/cm² was applied using a syringe pump for 1 min. Numbers of WT endothelial cells adhered to vitronectin under static condi‐tion per field was assigned the value of 100%, and relative adhesion was

calculated as described in Materials and methods. (D) Migration of WT and DiYF endothelial cells on various integrin ligands. Transwell tissue culture inserts were coated with various integrin ligands. WT and DiYF mouse lung ECs were seeded into the top chamber. Cells were allowed to migrate, and nonmigrated cells adhered to the top surface were removed. The number of WT cells that migrated onto the vitronectin-coated insert was assigned a value of 100% (*, P = 0.00004). (E) VEGF-induced migration of WT and DiYF mouse lung ECs. The migration assay was performed as described in Materi‐als and methods using vitronectin as a substrate. The number of WT ECs that migrated in the absence of VEGF was assigned a value of 100%. (F and G) Reduced migration of DiYF endothelial cells on β₃ integrin ligand. WT and DiYF ECs were serum starved and wounded across the cell monolayer by scraping away a swath of cells. The wound sites were photographed imme‐diately (time zero) and 12 h later (*, P = 0.00004). The data represent the results of three independent experiments. Bar, 220 μm.
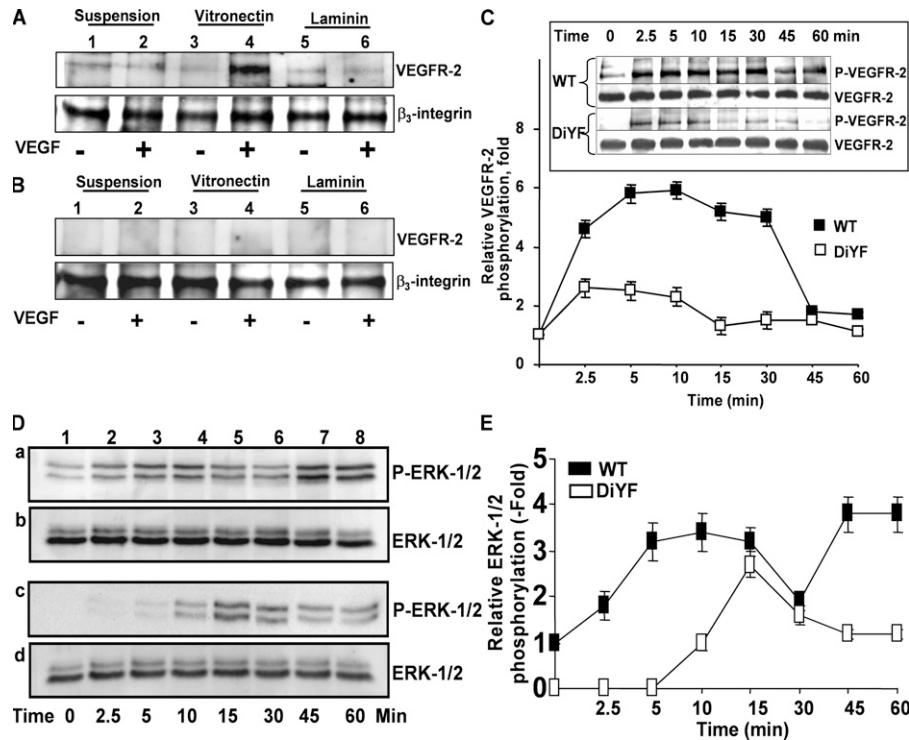
Figure 6. **β₃ integrin cytoplasmic tyrosine residues are required for VEGF–induced VEGFR–2 and β₃ integrin interaction.** WT (A) and DiYF (B) mouse lung endothelial cells were kept in suspension (lanes 1 and 2) or plated on vitronectin-coated (lanes 3 and 4) or laminin-coated (lanes 5 and 6) plates. These cells were treated with VEGF for 15 min (lanes 2, 4, and 6), and cells were lysed, immunoprecipitated with anti–β₃ integrin antibody, and analyzed by Western blot using anti–VEGR-2 antibody. The same blots were reprobed with rabbit anti–mouse β₃ integrin antibody to conform equal loading (A and B, bottom). (C and E) Mutation of β₃ integrin tyrosines 747 and 759 impairs VEGF-induced VEGFR-2 phosphorylation and down-stream target molecules. WT and DiYF mouse lung endothelial cells were induced with 20 ng/ml VEGF for 0–60 min at 37°C. Cells lysates were im-munoprecipitated with anti–VEGR-2 antibody and analyzed by Western blot using an antiphosphotyrosine antibody. The same blots were reprobed with anti–VEGR-2 antibody as loading control. Cell lysates were also ana-lyzed by Western blot using an anti-p-ERK-1/2 antibody (D, a and c). The same blots were reprobed with anti–ERK-1/2 antibody as loading control (D, b and d). Densities of the bands were detected, and fold changes over control were calculated and represented in the graph (E). The data points represent mean ± SD of samples from three separate experiments.

events downstream of VEGFR–2. To further examine this phenomenon WT and DiYF cells were induced with VEGF for various time periods and cell lysates were analyzed for phosphorylation of extracellular signal–regulated kinase (ERK)-1/2 as downstream target molecule of VEGFR-2. In WT ECs, VEGF induced strong bell-shaped response with a 3.5-fold increase in ERK-1/2 phosphorylation relative to unstimulated cells within 2.5 to 15 min. In contrast, the max-imum ERK-1/2 phosphorylation in DiYF ECs upon VEGF stimulation was only 2.5-fold over control and appeared only after 15 min of VEGF stimulation. Importantly, VEGFR-2–mediated ERK-1/2 phosphorylation was immediate and lon-ger in WT ECs than in DiYF ECs (Fig. 6, D and E).

β₃ integrin cytoplasmic tyrosine motifs are critical for VEGF–induced α$_v$β₃ integrin activation

An intrinsic property of integrin is an increase in soluble li-gand binding in response to stimulation, a process referred to as integrin activation. We and others previously reported that VEGF activates α$_v$β₃ integrin on ECs in response to VEGF

(24). We sought to determine whether impaired activation of VEGFR–2 in DiYF ECs resulted in defective α$_v$β₃ activa-tion by VEGF. VEGF induced a sixfold increase of fibrinogen binding to WT ECs, but only a threefold increase in binding to DiYF ECs (Fig. 7 A). MnCl₂, an agonist known to acti-vate integrins and stimulate β₃ integrin tyrosine phosphory-lation (25), produced at least a 12-fold increase in fibrinogen binding to WT ECs compared with a 5-fold increase ob-served in DiYF ECs (Fig. 7 B). The specificity of ligand binding was confirmed by addition of 10-fold excess of unlabeled fibrinogen. Similar results were observed when in-tegrin activation was monitored using a monovalent activation-dependent ligand WOW-1 Fab. VEGF and MnCl₂ stimulated 9- and 11-fold increases, respectively, in WOW-1 binding to WT ECs and 3.5- and 4-fold increases, respectively, to DiYF ECs (Fig. 7 C and Fig. 6 D). Thus, it is apparent that the mutations within the cytoplasmic domain of β₃ in-tegrin in the DiYF mice significantly impair the process of integrin activation, resulting in defective cell adhesion and migration.

DISCUSSION

To investigate the role played by β_3 integrin in pathological angiogenesis, we replaced the WT β_3 integrin with a mutated form unable to undergo phosphorylation, creating the knock-in mouse DiYF. The mutant β_3 integrin is expressed and is present on cell surfaces at the normal levels, but is defective in signaling. The major advantage of this model is that it allows monitoring of $\alpha_V\beta_3$ function in primary endothelial cells as opposed to model cell lines lacking appropriate receptors and signaling intermediates. The ex vivo and in vitro results from this model provided novel information that is different from the previously published results from in vitro studies and β_3 knockout mice experiments (8). A unique aspect of our experimental system is that compensatory or over-compensatory responses were not observed; these responses often occur in knockout models when a protein of interest is absent during development (26). Using DiYF knock-in mice, we assessed pathological neovascularization in vivo and performed an extensive analysis of the underlying mechanisms of angiogenesis using ex vivo models. The major

findings of this paper are the following. (a) Phosphorylation of β_3 integrin in WT ECs occurred in response to integrin ligation and VEGF stimulation. (b) Lack of β_3 integrin phosphorylation in DiYF knock-in mice resulted in impaired angiogenic response in three distinct in vivo models. As a result of reduced vascularization, tumor growth was significantly inhibited in DiYF mice compared with WT. (c) At the same time, DiYF mutation did not affect embryogenesis, organogenesis, and overall vascular development. In contrast to the phenotype of β_3 integrin knockout mice, DiYF pups were broadly normal and did not show any hemorrhage in any organ. Vascular density and maturation in adult DiYF animal was also normal, indicating that integrin phosphorylation is crucial for pathological but not normal vascularization. (d) In ECs from DiYF mice, VEGF-induced functional responses (cell adhesion, spreading, migration, and capillary tube formation) were defective compared with WT. (e) Lack of β_3 integrin phosphorylation in DiYF ECs lead to disruption of the VEGFR-2–β_3 integrin complex and lack of VEGFR-2 phosphorylation in response to VEGF. (f) VEGF-induced integrin activation (inside-out signaling) was suppressed in DiYF ECs compared with WT ECs.

Our data show that, in WT ECs, phosphorylation of β_3 integrin occurs in response to integrin ligation and VEGF stimulation. The finding that β_3 phosphorylation occurs not only in response to adhesion to extracellular matrix (i.e., as a result of outside-in integrin signaling), but also upon treatment with VEGF, indicates that β_3 might play an important regulatory role in outside-in integrin signaling, also known as integrin activation. In DiYF ECs, β_3 cannot be phosphorylated, and integrin activation, as measured by soluble ligand binding to $\alpha_V\beta_3$, was considerably reduced compared with WT. Previous studies demonstrated that ligation or the treatment with the agonist Mn^{2+} induces β_3 integrin phosphorylation in cells other than ECs (25). At the molecular level, it was also shown that β_3 integrin phosphorylation controls the strength of receptor–ligand interaction (27), and might contribute to the overall functional activity of the integrin.

In three distinct models, one that measured capillary formation in Matrigel and two others for vascularity of implanted tumors, we observed that pathological angiogenesis was severely impaired in DiYF mice. Our findings are consistent with the results of studies using $\alpha_V\beta_3$ blocking antibodies and demonstrate a key role for $\alpha_V\beta_3$ integrin in angiogenesis, suggesting that β_3 integrin is a positive regulator of angiogenesis and its phosphorylation is a critical step in EC responses during VEGF-induced neovascularization. Further, our findings provide an additional argument that increased angiogenesis observed in β_3 knockout mice (8) is a result of molecular compensation via VEGR-2; this emphasizes the physiological importance of VEGR-2–$\alpha_V\beta_3$ cross-regulation in ECs, but does not reflect the true function of $\alpha_V\beta_3$ integrin in angiogenesis in an organism expressing normal amounts of this receptor. Since our experimental approach does not involve a complete deletion of β_3 integrin from the cell surface, it does not trigger compensatory responses (i.e., up-regulation of
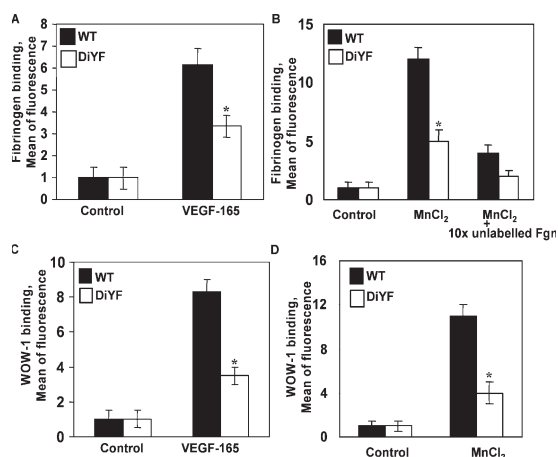
Figure 7. β_3 integrin phosphorylation controls integrin activation. DiYF ECs exhibited reduced fibrinogen binding in response to growth factors. WT and DiYF mouse lung ECs were serum starved for 4 h and washed twice with PBS. These cells were incubated with FITC fibrinogen in the presence or absence of 20 ng/ml VEGF for 45 min at 37°C. Cells were fixed, washed, and analyzed by flow cytometry. Bars represent mean fluorescence intensity of three independent experiments performed in triplicates (A). WT and DiYF mouse lung endothelial cells were stimulated with 1 mM $MnCl_2$. $MnCl_2$-induced fibrinogen binding was diminished by 10-fold excess of unlabeled fibrinogen showing specificity of binding (B). (C and D) β_3 integrin cytoplasmic tyrosine motif is essential for interaction with monovalent ligand WOW-1 Fab. WT and DiYF mouse lung endothelial cells were serum starved for 4 h, washed twice with PBS, and incubated with WOW-1 Fab in the presence or absence of 20 ng/ml VEGF for 45 min at 37°C. Cells were washed and incubated with FITC-conjugated goat anti–mouse IgG for 30 min at room temperature. Cells were fixed with 0.4% formaldehyde, washed, and analyzed by flow cytometry. Bars represent mean fluorescence intensity of three independent experiments performed in triplicates (C). WT and DiYF mouse lung endothelial cells were also induced with 1 mM $MnCl_2$ as positive control (D). Asterisks indicates significant difference between WT and DiYF endothelial cells ($P < 0.05$).

VEGR–2). The phenomenon of molecular compensation—in many cases, over-compensation—in knockout mice has been described in numerous reports and represents a major drawback of the knockout approach. Frequently, the loss of a particular protein results in increased expression of other members of the same family, revealing the functional redundancy (28). It has been shown, for example, that $\alpha_V\beta_5$ integrin can compensate for the loss of $\alpha_5\beta_1$ integrin (26). Analysis of the substitute molecule, which is structurally and functionally distinct from the targeted protein (29, 30), might reveal new connections within the molecular network. It is intriguing that VEGR–2, a tyrosine kinase receptor, can compensate for the loss of a member of integrin family of cell adhesion molecules, as VEGR–2 is distinct in regard to ligand repertoire and other functional aspects.

In the present study, impaired angiogenesis in DiYF knock-in mice resulted from the decreased adhesion, spreading, and migration of ECs in response to VEGF. Interestingly, impaired cell adhesion and migration was observed only on vitronectin as a substrate, but not on fibronectin or collagen. Nevertheless, ex vivo angiogenesis in Matrigel, and in vivo angiogenesis, was defective, emphasizing a role for $\alpha_V\beta_3$ in this process. At the molecular level, this study demonstrated that impaired tyrosine phosphorylation of β_3 integrin in DiYF ECs abrogated $\alpha_V\beta_3$–VEGFR–2 complex formation and resulted in dramatically reduced phosphorylation of VEGFR–2 upon VEGF stimulation. Since VEGF (via VEGFR–2 as its major functional receptor on ECs) induces phosphorylation of $\alpha_V\beta_3$ and phosphorylation of $\alpha_V\beta_3$, in turn, is required for complete and sustained phosphorylation of VEGFR–2, it can be concluded that these two receptors are able to cross-activate each other in ECs, therefore forming a functional partnership that is essential for successful angiogenesis.

Collectively, our findings demonstrate that $\alpha_V\beta_3$ and its inside–out and outside–in signaling is essential for pathological angiogenesis and undoubtedly represents a promising target for pharmaceutical approaches. However, when developing new inhibitors for angiogenesis, one should take into consideration the complexity of $\alpha_V\beta_3$ regulation, its interactions with other receptors, and possible compensatory changes resulting from its suppression.

MATERIALS AND METHODS

Animals. DiYF mice were generated in the laboratory of Dr. David R. Phillips and maintained on a C57/Bl6 background (seven generations of backcrossing). 6–8-wk-old WT and DiYF mice were used in our study. We performed all procedures according to protocols approved by Cleveland Clinic Foundation Institutional Animal Care and Use Committee.

In vivo Matrigel plug assay. WT and DiYF animals received an abdominal subcutaneous injection of 500 µl Matrigel mixed with VEGF (60 ng/ml) and heparin (60 units/ml). After 7 d, the animals were killed and dissected. Matrigel plugs were removed and digested using 5 ml Drabkin reagent, and quantification of neovascularization was assessed using a hemoglobin assay as per the manufacturer's protocol.

Tumor angiogenesis. WT and DiYF mice were subcutaneously injected with freshly harvested 10^6 B16F10 mouse melanoma or RM-1 mouse prostate cancer cells. Tumors were collected 10 d after injection and tumor weights were measured. Tumors were also photographed and processed for immunohistochemical staining.

Immunohistochemistry and image analysis. Immunohistochemistry and image analysis was performed as described previously (21). Matrigel plugs or tumor tissues sections were stained with polyclonal rabbit anti-vWF antibody (Abcam, Inc.) or rat anti-F4/80 (Serotec, Inc). Sections were counterstained with hematoxylin. WT and DiYF skin, liver, and kidney tissue samples were processed and stained for vWF or laminin. B16F10 tumor sections were stained with polyclonal anti-CD31 (Fitzgerald Industries Intl.) and anti-laminin (Sigma-Aldrich) antibody.

Aortic ring assay and isolation of endothelial cells. The mouse aortic ring assay was performed as described previously (21). WT and DiYF mouse lungs were excised, minced, and digested using collagenase-dispase reagent (3 mg/ml). Digests were strained and the resulting cell suspension was plated on flasks coated with 1 mg/ml fibronectin. Endothelial cells were isolated and characterized as described previously (31).

Cell adhesion and cell spreading assay. The cell adhesion assay was performed as described previously (32). Mouse lung endothelial cell suspensions were added to ligand-coated wells and placed in humidified incubator for 45 min. The wells were gently washed three times with DMEM and photographs were taken. The numbers of attached and spread cells per field were counted. Adhesion assay under shear stress conditions was performed as described previously (33). Prior to the beginning of the experiment WT and 2.25-fold excess DiYF endothelial cells were added on vitronectin-coated coverslips to achieve approximately equal number of adherent cell population and allowed to interact with the matrix for 15 min. These coverslips were gently washed and introduced into the bottom of the flow chamber. Shear stress of 5–30 dyne/cm^2 was applied using syringe pump for 1 min. Number of WT endothelial cells adhered to vitronectin under static condition per field was assigned the value of 100% and relative adhesion was calculated.

Endothelial cell migration and wound healing assay. Endothelial cell migration assay was performed as described previously (24). WT and DiYF mouse lung endothelial cells were grown to confluence in 12-well plates precoated with various integrin ligands. Cells were serum starved and then a wound was created. Images were recorded immediately after wounding (time zero) and 12 h later. Cell migration was quantified using image analysis of five randomly selected fields of denuded area. The mean wound area is expressed as percent of recovery (% R) from three identically treated plates using the equation % R = $[1 - (T_t/T_0)] \times 100$, where T_0 is the wounded area at 0 h and T_t is the wounded area after 12 h.

WOW-1 and fibrinogen binding assay. WOW-1 Fab binding assay was performed as described previously (34). To assess fibrinogen binding, WT and DiYF mouse lung endothelial cells were serum starved for 4 h and further induced with 20 ng/ml VEGF-165 or 1 mm $MnCl_2$. FITC-labeled fibrinogen was added at a final concentration of 200 nM for 45 min. Cells were fixed and washed twice with ice-cold PBS. FACS was performed using a FACS Calibur (Becton Dickinson), and data were analyzed using Cell-Quest software program.

Endothelial tube and precapillary cord formation assay. The formation of vascular tube-like structures by WT and DiYF mouse lung endothelial cells were assessed on the basement membrane matrix preparation. WT and DiYF mouse lung endothelial cells were seeded on Matrigel-coated plates. Medium with or without 20 ng/ml VEGF was added, and cells were further incubated at 37°C for 8 h. The tube formation was observed using an inverted phase–contrast microscope, and photographs were taken from each well. Using ImagePro software, the degree of tube formation was quantified by measuring the length of tubes in random fields. The precapillary cord formation assay was performed as described previously (22).

Immunoprecipitation and Western blot analysis. Immunoprecipitation was performed as described previously (23). To analyze the β_3 integrin tyrosine phosphorylation of WT and DiYF mouse lung microvascular endothelial cells, ECs were added to various integrin ligand-coated plates and incubated at 37°C for 60 min. Cell lysates containing equal amount of proteins were subjected to Western blot analysis using rabbit anti–integrin β_3 [pY^{747}] and [pY^{759}] antibody (Biosource International, Inc). Cell lysates were also analyzed for β_3 integrin expression as a loading control. Serum-starved WT and DiYF ECs were also treated with 20 ng/ml VEGF for 0–60 min. Cell lysates were analyzed by Western blot using anti–integrin β_3 [pY^{747}], anti–integrin β_3 [pY^{759}], anti–ERK-1/2 and anti–p-ERK-1/2 (Cell Signaling Technology) antibodies.

Statistical analysis. Values were expressed as mean ± SDs. p values were based on the paired t test. Results were considered statically significant with $P < 0.05$.

REFERENCES

1. Eliceiri, B.P. 2001. Integrin and growth factor receptor crosstalk. *Circ. Res.* 89:1104–1110.
2. Friedlander, M., P.C. Brooks, R.W. Shaffer, C.M. Kincaid, J.A. Varner, and D.A. Cheresh. 1995. Definition of two angiogenic pathways by distinct alpha v integrins. *Science.* 270:1500–1502.
3. Brooks, P.C., R.A. Clark, and D.A. Cheresh. 1994. Requirement of vascular integrin alpha v beta 3 for angiogenesis. *Science.* 264:569–571.
4. Brooks, P.C., S. Stromblad, R. Klemke, D.Visscher, F.H. Sarkar, and D.A. Cheresh. 1995. Antiintegrin alpha v beta 3 blocks human breast cancer growth and angiogenesis in human skin. *J. Clin. Invest.* 96:1815–1822.
5. Drake, C.J., D.A. Cheresh, and C.D. Little. 1995. An antagonist of integrin alpha v beta 3 prevents maturation of blood vessels during embryonic neovascularization. *J. Cell Sci.* 108(Pt 7):2655–2661.
6. Hammes, H.P., M. Brownlee, A. Jonczyk, A. Sutter, and K.T. Preissner. 1996. Subcutaneous injection of a cyclic peptide antagonist of vitronectin receptor-type integrins inhibits retinal neovascularization. *Nat. Med.* 2:529–533.
7. Brooks, P.C., A.M. Montgomery, M. Rosenfeld, R.A. Reisfeld, T. Hu, G. Klier, and D.A. Cheresh. 1994. Integrin alpha v beta 3 antagonists promote tumor regression by inducing apoptosis of angiogenic blood vessels. *Cell.* 79:1157–1164.
8. Reynolds, L.E., L. Wyder, J.C. Lively, D. Taverna, S.D. Robinson, X. Huang, D. Sheppard, R.O. Hynes, and K.M. Hodivala-Dilke. 2002. Enhanced pathological angiogenesis in mice lacking beta3 integrin or beta3 and beta5 integrins. *Nat. Med.* 8:27–34.
9. Robinson, S.D., L.E. Reynolds, L. Wyder, D.J. Hicklin, and K.M. Hodivala-Dilke. 2004. Beta3-integrin regulates vascular endothelial growth factor-A-dependent permeability. *Arterioscler. Thromb. Vasc. Biol.* 24:2108–2114.
10. Hodivala-Dilke, K.M., A.R. Reynolds, and L.E. Reynolds. 2003. Integrins in angiogenesis: multitalented molecules in a balancing act. *Cell Tissue Res.* 314:131–144.
11. Sheppard, D. 2002. Endothelial integrins and angiogenesis: not so simple anymore. *J. Clin. Invest.* 110:913–914.
12. Cheresh, D.A., and D.G. Stupack. 2002. Integrin-mediated death: an explanation of the integrin-knockout phenotype? *Nat. Med.* 8:193–194.
13. Hynes, R.O. 2002. Integrins: bidirectional, allosteric signaling machines. *Cell.* 110:673–687.
14. Chandhoke, S.K., M. Williams, E. Schaefer, L. Zorn, and S.D. Blystone. 2004. Beta 3 integrin phosphorylation is essential for Arp3 organization into leukocyte alpha V beta 3-vitronectin adhesion contacts. *J. Cell Sci.* 117:1431–1441.
15. Butler, B., M.P. Williams, and S.D. Blystone. 2003. Ligand-dependent activation of integrin alpha vbeta 3. *J. Biol. Chem.* 278:5264–5270.
16. Law, D.A., F.R. DeGuzman, P. Heiser, K. Ministri-Madrid, N. Killeen, and D.R. Phillips. 1999. Integrin cytoplasmic tyrosine motif is required for outside-in alphaIIbbeta3 signalling and platelet function. *Nature.* 401:808–811.
17. Prasad, K.S., P. Andre, M. He, M. Bao, J. Manganello, and D.R. Phillips. 2003. Soluble CD40 ligand induces beta3 integrin tyrosine phosphorylation and triggers platelet activation by outside-in signaling. *Proc. Natl. Acad. Sci. USA.* 100:12367–12371.
18. Das, R., G.H. Mahabeleshwar, and G.C. Kundu. 2004. Osteopontin induces AP-1-mediated secretion of urokinase-type plasminogen activator through c-Src-dependent epidermal growth factor receptor transactivation in breast cancer cells. *J. Biol. Chem.* 279:11051–11064.
19. Sundberg, C., and K. Rubin. 1996. Stimulation of beta1 integrins on fibroblasts induces PDGF independent tyrosine phosphorylation of PDGF beta-receptors. *J. Cell Biol.* 132:741–752.
20. Eliceiri, B.P., and D.A. Cheresh. 1999. The role of alphav integrins during angiogenesis: insights into potential mechanisms of action and clinical development. *J. Clin. Invest.* 103:1227–1230.
21. Chen, J., P.R. Somanath, O. Razorenova, W.S. Chen, N. Hay, P. Bornstein, and T.V. Byzova. 2005. Akt1 regulates pathological angiogenesis, vascular maturation and permeability in vivo. *Nat. Med.* 11:1188–1196.
22. Hoang, M.V., M.C. Whelan, and D.R. Senger. 2004. Rho activity critically and selectively regulates endothelial cell organization during angiogenesis. *Proc. Natl. Acad. Sci. USA.* 101:1874–1879.
23. Soldi, R., S. Mitola, M. Strasly, P. Defilippi, G. Tarone, and F. Bussolino. 1999. Role of alphavbeta3 integrin in the activation of vascular endothelial growth factor receptor-2. *EMBO J.* 18:882–892.
24. Byzova, T.V., C.K. Goldman, N. Pampori, K.A. Thomas, A. Bett, S.J. Shattil, and E.F. Plow. 2000. A mechanism for modulation of cellular responses to VEGF: activation of the integrins. *Mol. Cell.* 6:851–860.
25. Blystone, S.D., M.P. Williams, S.E. Slater, and E.J. Brown. 1997. Requirement of integrin beta3 tyrosine 747 for beta3 tyrosine phosphorylation and regulation of alphavbeta3 avidity. *J. Biol. Chem.* 272:28757–28761.
26. Yang, J.T., and R.O. Hynes. 1996. Fibronectin receptor functions in embryonic cells deficient in alpha 5 beta 1 integrin can be replaced by alpha V integrins. *Mol. Biol. Cell.* 7:1737–1748.
27. Boettiger, D., F. Huber, L. Lynch, and S. Blystone. 2001. Activation of alpha(v)beta3-vitronectin binding is a multistage process in which increases in bond strength are dependent on Y747 and Y759 in the cytoplasmic domain of beta3. *Mol. Biol. Cell.* 12:1227–1237.
28. Tedford, K., L. Nitschke, I. Girkontaite, A. Charlesworth, G. Chan, V. Sakk, M. Barbacid, and K.D. Fischer. 2001. Compensation between Vav-1 and Vav-2 in B cell development and antigen receptor signaling. *Nat. Immunol.* 2:548–555.
29. Allikian, M.J., A.A. Hack, S. Mewborn, U. Mayer, and E.M. McNally. 2004. Genetic compensation for sarcoglycan loss by integrin alpha7beta1 in muscle. *J. Cell Sci.* 117:3821–3830.
30. Stromblad, S., A. Fotedar, H. Brickner, C. Theesfeld, d.D. Aguilar, M. Friedlander, and D.A. Cheresh. 2002. Loss of p53 compensates for alpha v-integrin function in retinal neovascularization. *J. Biol. Chem.* 277:13371–13374.
31. Fan, J., R.S. Frey, A. Rahman, and A.B. Malik. 2002. Role of neutrophil NADPH oxidase in the mechanism of tumor necrosis factor-alpha-induced NF-kappa B activation and intercellular adhesion molecule-1 expression in endothelial cells. *J. Biol. Chem.* 277:3404–3411.
32. Byzova, T.V., and E.F. Plow. 1998. Activation of alphaVbeta3 on vascular cells controls recognition of prothrombin. *J. Cell Biol.* 143:2081–2092.
33. Ahrens, I.G., N. Moran, K. Aylward, G. Meade, M. Moser, D. Assefa, D.J. Fitzgerald, C. Bode, and K. Peter. 2006. Evidence for a differential functional regulation of the two beta(3)-integrins alpha(V)beta(3) and alpha(IIb)beta(3). *Exp. Cell Res.* 312:925–937.
34. Pampori, N., T. Hato, D.G. Stupack, S. Aidoudi, D.A. Cheresh, G.R. Nemerow, and S.J. Shattil. 1999. Mechanisms and consequences of affinity modulation of integrin alpha(V)beta(3) detected with a novel patch-engineered monovalent ligand. *J. Biol. Chem.* 274:21609–21616.